High-temperature resistance of the $YBa_2Cu_3O_{6+x}$ tetragonal phase

M. Affronte, E. Minghini, C. Nobili, and G. Ottaviani
Istituto Nazionale per la Fisica della Materia and Dipartimento di Fisica, Università di Modena, via G. Campi 213/A, 41100 Modena, Italy

L. Bonoldi and M. Sparpaglione
Istituto Guido Donegani, Via S. Salvo, 20097 San Donato, Italy

F. Licci
Istituto Materiali Speciali per l'Elettronica e Magnetismo del Consiglio Nazionale delle Ricerche, via Chiavari 18/A, 43100 Parma, Italy

(Received 4 December 1995; revised manuscript received 1 April 1996)

We have studied the resistance behavior of tetragonal $YBa_2Cu_3O_{6+x}$ (YBCO with $x<0.5$) at high temperatures. Resistance measurements were performed following different thermal procedures in flowing Ar atmosphere. Measurements taken during slow heating exhibit a maximum in the temperature dependence of resistance (R vs T). The temperature at which this maximum occurs systematically shifts towards lower temperatures as the sweeping rate decreases. In the limit of vanishing sweeping rate, i.e., when the steady state resistance is measured after long ($\sim 10^3$ min) isothermal heat treatment, the R vs T curve exhibits a maximum at ~650 °C. Resistance measurements taken during slow cooling (0.1–0.5 °C/min) generally depend on the thermal cycle. Weight measurements were used to evaluate the effects of the change of oxygen stoichiometry in different experiments. The comparison of resistance and weight measurements shows that bulk oxygen diffusion occurs in a time scale much shorter (~30 min at 650 °C) than resistance relaxation ($\sim 10^3$ min at 650 °C). We propose that the long relaxation time observed in resistivity measurements, similarly to other time dependent phenomena reported in the literature, is related to ordering (or disordering) of oxygen defects and we conclude that the resistance maximum at 650 °C mainly reflects different oxygen configurations achieved above 500 °C. [S0163-1829(96)07633-3]

INTRODUCTION

It is generally accepted that tetragonal $YBa_2C_3O_{6+x}$ (YBCO with $0<x<0.5$) is a semiconductor. The characterization of this semiconductor, however, is not definitively established especially for what concerns the electronic properties. Optical measurements[1] have shown that the characteristic energy gap is 1.7 eV. It has been found that tetragonal $YBa_2C_3O_{6+x}$ with $0<x<0.4$ orders in a antiferromagnetic state below ~400 K although the effects of this transition on the electronic transport properties have not been clearly shown yet. Electronic transport properties of tetragonal $YBa_2Cu_3O_{6+x}$ have been reported by several authors.[2–11] A resistance decrease with increasing temperature has been found at high temperatures as the oxygen content is reduced below 6.5 per u.f. (Ref. 6). Freitas and Plaskett gave a data interpretation in the framework of a conventional band scheme.[6] Genossar *et al.* interpreted the high-temperature resistance within a narrow band picture,[7] while Yoo[10] discussed it in terms of polaron conduction. However, the spread of data is quite large in the literature and we note, for instance, that there is no general agreement on the charge transport activation energy of the semiconducting YBCO.

High-temperature resistance data are found to be scarcely reproducible. Actually, most of the authors reported that a ''... long time is required to get a steady voltage...'' although this ''long time'' was a few hours for somebody and a few days for someone else. This behavior was generally considered as a spurious effect and shortly discussed. However, it is remarkable that if one keeps a sample of the orthorhombic YBCO phase in flowing oxygen at high temperature, one gets almost immediately a steady resistance, while if the same specimen is driven into the tetragonal phase and kept in inert gas atmosphere it takes several days to get a steady electrical signal.[12] On the other hand, in the last few years there were several reports on time-dependent phenomena observed on oxygen-deficient YBCO. A change of the superconducting transition temperature T_c was observed when a $YBa_2Cu_3O_{6.4}$ sample is heated from T_c to room temperature.[13] Photoinduced changes on the electronic properties of $YBa_2Cu_3O_{6.4}$ have been observed as well.[14–16] Compared studies of resistance and neutron diffraction on $YBa_2Cu_3O_{6.25}$ powders suggest that electrical changes can be related to an oxygen ordering process.[17] Theoretical studies[18] have recently pointed out that a large variety of metastable phases can be formed with different local oxygen ordering. Moreover, they found an intimate relationship between the oxygen ordering and the electronic properties of the nonstoichiometric YBCO.[19] Despite that, a wide region of the YBCO phase diagram is still experimentally unexplored. In particular little work has been done in order to see whether time-dependent phenomena occur at high temperatures, i.e., in the phase diagram region that is the most favorable for the formation of metastable phases.

The aim of this work is twofold: (1) to clarify to what extent it is possible to observe a reproducible high-

temperature resistance behavior; (2) to see whether and how time-dependent phenomena occur above room temperature. In particular, we have studied the resistance behavior under different and well-defined procedures, i.e., upon heating and cooling at different rates. These results are compared with the resistance values obtained at the end of isothermal treatments. Thermogravimetric measurements were also taken using the same procedures in order to clarify the effects of bulk oxygen loss.

SAMPLE PREPARATION AND EXPERIMENTAL TECHNIQUES

$YBa_2Cu_3O_{6+x}$ was synthesized starting from CuO, $BaCO_3$, and Y_2O_3. Powders were mixed and milled in stoichiometric proportions and then several heat treatments were performed. The first one was carried out in oxygen atmosphere at 940 °C for 12 h; the resulting powder was grounded and reacted again under the same conditions for 36 h. This last cycle was repeated two more times. Pellets of 13 mm diameter and 1.6 mm thickness were then done, heated at 920 °C for 16 h and annealed in flowing oxygen at 450 °C for 24 h. The oxygen content was $6.94+0.03$ per u.f. It was determined by dissolving a pellet in nitric acid and measuring the total oxygen developed as a free gas with a Danny 8400 gas chromatography.[20] The x-ray-diffraction pattern was made with a Philips WP 1830 powder diffractometer with Cu $K\alpha$ radiation. The observed peaks were all assigned to the orthorhombic YBCO compound spectra, no spurious lines were found.

The material is polycrystalline. Scanning electron micrographs (SEM), made with a Jeol JSM-820 microscope, show a lamellar growth with grains of typical (ab plane) size of 20 μm. The material is porous, holes are present, and the sample average density is between 4.1 and 4.6 g/cm^3. The samples have a room-temperature resistivity of 1–3 mΩ cm; the superconducting transition temperature obtained by sheet resistance measurements is 91.5 K.

In situ resistance measurements were performed using a four-probe method in the van der Pauw configuration with silver contacts, spring loaded on small gold dots deposited by sputtering onto the oxide. Contacts were tested for ohmic behavior by reversing the current polarity; ohmic checks were also performed during the heat treatments.

RESULTS

In order to measure the high-temperature resistivity of tetragonal YBCO we first need to reduce the oxygen content from 7 to 6.2–6.1 per u.f., then the actual resistance measurement is performed. These two steps were made in the same thermal cycle in our experiments by choosing the opportune ramps and plateau's and controlling the atmosphere during the thermal cycle. Finally measurements of the temperature dependence of resistance were performed during heating and cooling ramps or isothermal heat treatments.

In the first set of experiments, the procedure used for resistance and weight measurements was the following: the sample was quickly heated (rate 10 °C/min) in oxygen atmosphere up to 400 °C then the atmosphere was changed to argon and the heating rate was set to a given value (between

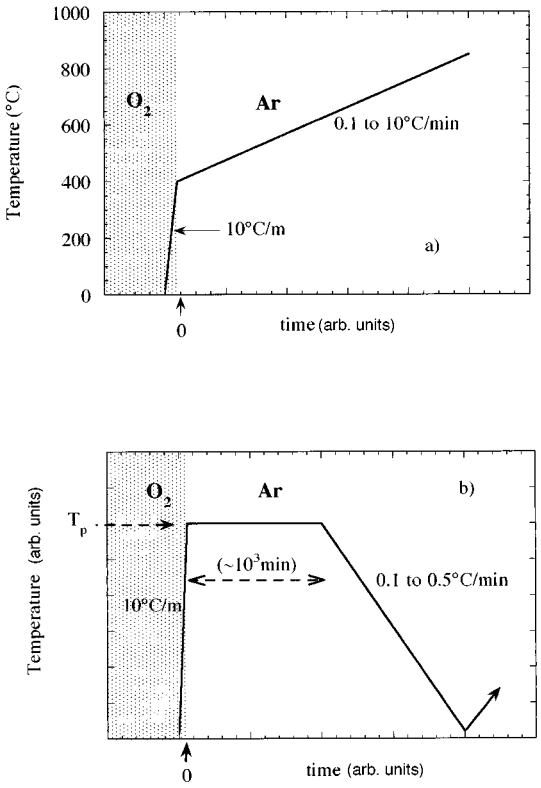

FIG. 1. Heat treatment procedures used in our experiments.

0.1 to 10 °C/min depending on the experiment) and the heating continued up to 820 °C, see Fig. 1(a). The argon flow (purity=99.999%) can be considered equivalent to <10 ppm (1 Pa) oxygen partial pressure.

In Fig. 2 are presented the *in situ* resistance measurements

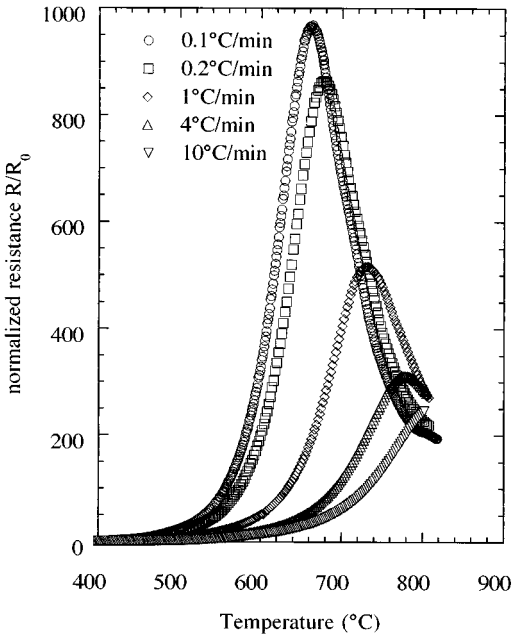

FIG. 2. Normalized sheet resistance values as a function of temperature measured at various heating rates: the heating procedure used in this experiment was that represented in Fig. 1(a). R_0 is the resistance value measured at room temperature at the beginning of the heat treatment.

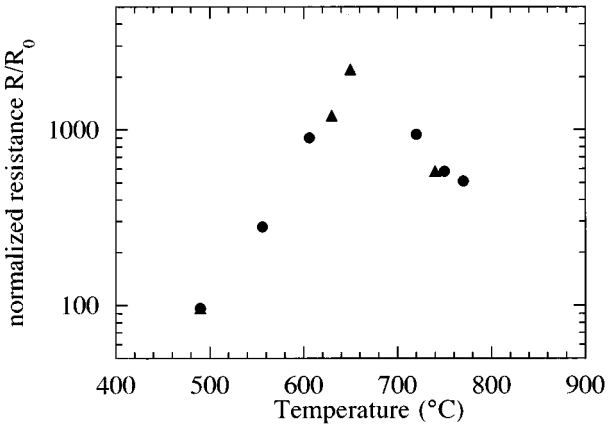

FIG. 3. Normalized sheet resistance as a function of temperature obtained at the end of isothermal annealing in argon atmosphere. R_0 is the resistance value measured at room temperature at the beginning of the heat treatment represented in Fig. 1(b). Different symbols indicate samples made by two different laboratories.

corresponding to various heating rates between 400 °C and 820 °C. The sheet resistance is normalized to R_0, the resistance measured at room temperature before any heat treatment. The starting-temperature of the horizontal axis, 400 °C, corresponds to the temperature at which the atmosphere was changed from oxygen to argon and the actual experiment begins.

We observe that all the curves have a similar shape although they were obtained at different heating rates. At the beginning, the sheet resistance grows with increasing temperature, then it reaches a maximum and finally it decreases with a further temperature increase. As the heating rate gets slower, the maximum value of the resistance $R_{\max}$ increases and the temperature $T_{\max}$ at which the maximum is reached shifts to lower values.

Resistance variation shown in Fig. 2 is due to a combination of the change of the oxygen stoichiometry and the temperature dependence of the resistance. In order to separate these two effects, we performed thermogravimetric measurements following the same heating treatment and environmental conditions, i.e., the heating treatment shown in Fig. 1(a). Such thermogravimetric analysis shows that the material does not suffer any detectable weight change in the first heating ramp under oxygen atmosphere up to 400 °C. Above 400 °C when the atmosphere was switched from oxygen to argon, we observed that the oxygen content reaches the value of 6.2 per u.f. as soon as the normalized resistance R/R_0 gets $\sim$100, almost independently to the heating rate. Reached this value, the oxygen content decreases only very slightly and it is not more detectable with our experimental sensitivity. However, weight measurements performed before and after the heating treatment indicate that the final oxygen concentration is $6.07+0.05$ per u.f. Thus in the last part of the heat treatment the oxygen content slightly changes between 6.2 to 6.1 per u.f.

In order to see to what extent the maximum in the R vs T curve is a feature of tetragonal YBCO, we report in Fig. 3 the resistance values obtained at the end of isothermal heat treatments in argon atmosphere. Namely the sample was heated up to a given temperature T_p at the rate of 10 °C/min in oxygen atmosphere, then the atmosphere was changed from oxygen to argon and the temperature was kept constant until we measured a steady resistance value, see Fig. 1(b). Typical relaxation times are of the order of days.[12] This procedure can be considered as a limiting case of experiments reported in Fig. 2, as isothermal treatments are equivalent to extremely slow heating rates. The set of data that we collected lies along a R vs T curve showing a maximum at about 650 °C. As expected, we observe that $T_{\max}$ and $R_{\max}$ of Fig. 3 (steady-state resistance) fits the general trend of curves of Fig. 2 (heating), namely $T_{\max}$ is the lowest and $R_{\max}$ is the highest one. Weight measurements performed at beginning and at the end of isothermal heat treatment show that the final oxygen content is 6.20 ± 0.05 per u.f. for T_p between 500 and 550 °C and 6.10 ± 0.05 per u.f. when $T_p \geqslant 600$ °C.

In a third set of experiments, we studied the R vs T behavior during cooling. Samples were first annealed in argon atmosphere following the procedure shown in Fig. 1(b) and for the time required to obtain final oxygen content between 6.1 and 6.2 per u.f. and a steady resistance value. The temperature dependence of the resistance was then measured during several slow cooling and heating processes taken at rates ranging from 0.1 to 0.5 °C/min. We note that the sweep temperature rate $\sim$0.5 °C/min are considered more than enough to get steady state in materials like silicides but also in oxygen-rich YBCO as we have shown in our previous work.[12] Results are plotted in Fig. 4(a) ($T_p=650$ °C) and 4(b) ($T_p=750$ °C). In these plots R_0 is the resistance value at the starting temperature, i.e., 650 °C and 750 °C, respectively. Resistance curves show a maximum occurring at temperatures between 500 °C and 650 °C and a minimum occurring between 300 °C and 500 °C. A further characteristic is the sharp discontinuity of the slope of the R vs T curves at about 130 °C ($\sim$400 K). In Fig. 4(c) we report data obtained in a short cycle up to 200 °C performed after heat treatment at 650 °C for 3000 min and slow cooling (0.5 °C/min). A sample was permanently kept in flowing Ar, never exposed to ambient during the whole heat treatment. In this case R_0 is the resistance at room temperature before the beginning of the short thermal cycle. The plot reported in Fig. 4(c) shows once more the discontinuity at $\sim$130 °C in the slope of the two different curves obtained during heating and cooling. We can consider that as one of the effects of the antiferromagnetic transition reported by several authors. The sharpness of the knee at $\sim$130 °C depends on the thermal cycle used in experiment. This suggests that the whole thermal cycle used to prepare samples is very important when one wants to study the antiferromagnetic state.

The most striking result, however, is the fact that the R vs T curve is not reproducible but it depends on the thermal cycle, see Fig. 4(b) and 4(c). In other words, the sample is not at equilibrium when temperature is swept even ''slowly.'' The following experiment may help to elucidate this point. Following the procedure described in Fig. 1(a), we heated the sample up to 400 °C in O_2, then we switched the atmosphere to Ar and we swept the temperature at 0.5 °C up to 709 °C and we maintained this temperature until a steady resistance was observed. After $\sim$2000 min the temperature was quickly increased up to 747 °C and the resistance was continuously monitored. Results are shown in Fig. 5. Thermogravimetric measurements, taken upon the same heat

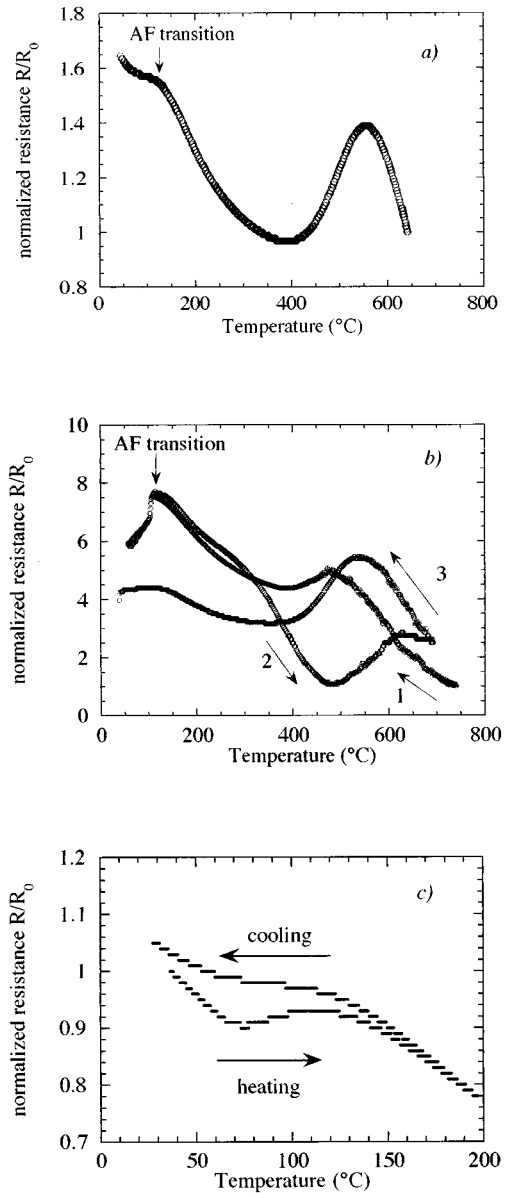

FIG. 4. Temperature dependence of the normalized resistance of YBCO. R_0 is the resistance value measured at the starting temperature, i.e., 650 °C, 750 °C, and 30 °C for (a), (b), and (c) respectively. (a) and (c): sample was previously treated at 650 °C in argon for 3000 min; (b): sample was treated at 750 °C for 2000 min following the heat treatment of Fig. 1(b). Measurements were taken during several cooling and heating cycles. Arrows and numbers show the thermal cycle path used during acquisition of resistance data. The sample was always kept in argon during these cycles.

treatment, show that there is no change of the bulk oxygen content, at least within our experimental accuracy, during the temperature change between 709 °C to 747 °C. Yet, we observe that it takes ~500 min to get a steady resistance value after the temperature change. Steplike temperature changes performed at lower temperatures show the same resistance relaxation occurring in time longer as the temperature decreases.

To get more insight on this long-time relaxation process we performed combined resistance and thermogravimetric (TGA) measurements. We followed the isothermal procedure of Fig. 1(b) with various T_p. Some characteristic curves

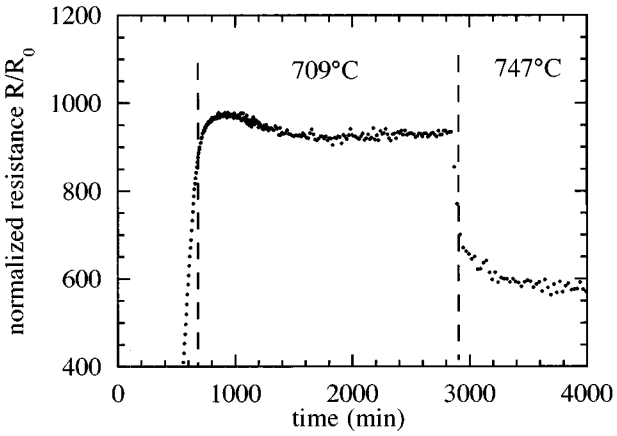

FIG. 5. Time evolution of the normalized resistance measured during steplike temperature change. R_0 is the initial resistance value measured at room temperature at the beginning of the heat treatment. The sample was first heated, following the procedure of Fig. 1(a), up to 709 °C and kept at this temperature for 2000 min, then temperature was suddenly increased up to 747 °C and kept for 1000 more mins. Note that it takes ~500 min to get a steady resistance value at 747 °C.

were already reported in our previous work,[21] here we briefly summarize a large data collection. Typical oxygen loss measured by TGA occurs in a time scale of 30 min at 650 °C, 80 min at 556 °C. The oxygen self-diffusion coefficient D_0 for YBCO at high temperatures for different oxygen nonstoichiometry has been reported by several authors.[22] Matsui *et al.*[23] reported that $D_0 \sim 4\times10^{-9}$ cm^2/s at 650 °C for an average oxygen content of 6.3 per u.f. Taking a typical grain size of $x \sim 20$ μm (typical dimensions of the ab plane for which oxygen diffusion is faster) we can estimate the oxygen diffusion time to be $t = x^2/D_0 \sim 17$ min in our case that is in good agreement we our TGA measurements at 650 °C. Although D_0 is a function of temperature and oxygen stoichiometry, we expect that this estimation provides the right order of magnitude for the oxygen diffusion in $YBa_2Cu_3O_{6.1}$, the actual material used in our experiments. The resistance measurement taken at the same conditions as TGA shows that an electrical steady state is achieved in a time scale of the order of 10^3 min, i.e., 2 orders of magnitude larger than the bulk diffusion of oxygen.

Grain size and material density play an important role in the determination of both diffusion and resistance relaxation time. Data presented so far refer to polycrystalline samples with a typical grain size of 20 μm (ab plane) and density ranging between 4.1 and 4.6 g/cm^3. We also performed resistance measurements on thin films and high-density ceramic (density >5.5 g/cm^3). In the latter case the time required to get steady resistance value increases up to one week at 650 °C. Note, however, that single grain cannot be considered isolated when the sample density is higher than 90–95% of the single-crystal density and therefore the bulk diffusion time increases too. Isothermal resistance measurements taken on thin films show that relaxation time is typically a factor 5–10 shorter than in pellets with density <5 g/cm^3. The time scale is still much higher than bulk oxygen diffusion.

X-ray studies were performed in order to see whether the

heat treatments provoke irreversible modifications in the material. X-ray-diffraction patterns were taken in samples quenched in different instants of the heat treatment of Fig. 1(a). X-ray-diffraction patterns show that at the beginning, when oxygen content is equal to 6.94 per u.f., the compound has orthorhombic symmetry. The orthorhombic-tetragonal transformation starts when the R/R_0 value is $\sim$10. For R/R_0 above 50 the material is completely tetragonal and it has also tetragonal symmetry at the end of the process. All the spectra lines which appear in the diffraction pattern can be assigned to the corresponding YBCO phase and no spurious phases were detected.

In a further experiment, sample heated with the procedure of Fig. 1(a) up to 820 °C in Ar atmosphere was subsequently exposed to oxygen for five minutes at 820 °C and then cooled in oxygen at 10 °C/min to room temperature. A large resistance decrease occurs when oxygen is introduced at 820 °C. At the end of the process, at room temperature, the value of R/R_0 is close to 1 and low-temperatures measurements show superconducting transition at $\sim$90 K. This indicates that, from the resistance point of view, the material is back to its original condition.

These experiments show that samples do not suffer irreversibly decomposition during our experiments. We mention, however, that the decomposition pressure for $RBa_2Cu_3O_{6+x}$ (R=rare earths) material was measured using a solid-state electrochemical cell.[8,11] If we take the nominal partial pressure of oxygen in our experiments (10 ppm$\sim$ 1 Pa) it turns out that the corresponding decomposition temperature is $\sim$700 °C in the phase diagram reported in Ref. 8 and 11. This contrasts with our observations that show no traces of spurious phases in sample treated in Ar flux up to 820 °C. Grader *et al.*[3] did not find sign of decomposition in samples treated in conditions similar to ours (820 °C in He atmosphere) in agreement with our observations. Note, moreover, that we found no discontinuity in the resistivity curves at 700 °C and the main features of the high-temperature resistivity that we report in this work are also observed in samples treated below 700 °C. This corroborates the fact that conditions used in our experiments are below the decomposition line of tetragonal YBCO. We ascribe the discrepancy with results reported in Ref. 8 and 11 to the different methods used to evaluate such low oxygen partial pressure in different experiments.

DISCUSSION

High-temperature resistance measurements in tetragonal YBCO were reported in the literature by several authors with a large data spread.[2–12] We have actually shown that measurements taken in dynamical conditions provide cycle-dependent curves [Fig. 4(b)] and steady-state resistance is obtained only keeping sample a few days at the same temperature (Fig. 5). When this procedure is used we obtain the plot of Fig. 3 that shows a maximum in the R vs T curve. Grader *et al.*[3] reported an identical behavior working in experimental conditions similar to ours. The presence of the R vs T maximum is also reported by Nowotny[11] and other groups[5,8,10] although the latter authors reported resistance curves as a function of pressure instead of temperature. Note that the height and the temperature at which the maximum occurs are the same in these independent experiments, indicating that preparation conditions and sample quality do not affect results once the sample density and the experimental procedure are the same. We may therefore conclude that the maximum in the R vs T curve is a genuine feature of the high-temperature resistivity of tetragonal YBCO obtained in very low oxygen partial pressure.

Curves reported in Fig. 2 are obtained in nonequilibrium conditions, although the sweeping temperature rates are quite slow. The R vs T data measured at a very slow sweeping rate 0.1 °C/min (this experiment lasted several days) is actually quite similar to that obtained in the steady state (Fig. 3) while the maximum in the R vs T curve is shifted towards higher temperatures as the temperature sweep rate increases. Briefly we may summarize our results in two main experimental facts: (1) Long relaxation time ($\sim 10^3$ min at 650 °C) is required in order to get electrical equilibrium at high temperatures; (2) the steady-state resistivity exhibits a maximum occurring at $\sim$650 °C in flowing inert gas.

In order to correlate the observed electronic properties with the structural features of oxygen-deficient YBCO, we briefly remind the reader of the main neutron-diffraction studies. It is known that YBCO undergoes an orthorhombic to tetragonal transition (in macroscopic scale) as soon as the oxygen content is lower than $\sim$6.4 per u.f. In an ideal tetragonal phase the oxygen of the basal plane is expected to equally distribute into the (1/2,0,0) and the (0,1/2,0) positions. Neutron studies have recently shown, however, that oxygen vacancies tend to distribute in a way not completely random. Radaelli *et al.*[24] have actually found that $YBa_2Cu_3O_{6+x}$ can best be described as a mixture of orthorhombic and tetragonal phases in the composition range $0.25 < x < 0.45$, while Sonntag and coworkers[25] reported evidences of superstructure due to oxygen defect ordering in $YBa_2Cu_3O_{6.35}$. We just mention here that we also found evidence of short-range oxygen order in $YBa_2Cu_3O_{6.2}$ obtained after long-time isothermal treatment at 490 °C by means of electron-diffraction patterns. It has been also pointed out that the orthorhombic to tetragonal transition is first order and metastable phases can coexist in several regions of the phase diagram depending on the thermal cycle used.[24] Based on these observations, we expect that the tetragonal side of the YBCO phase diagram is rich in metastable phases achieved under particular conditions (thermal path, annealing time, etc.) and characterized by different degrees of oxygen order. Further, Shaked and coworkers[17] have shown, by combined resistivity and neutron-diffraction measurements at room temperature, that the electronic properties of $YBa_2Cu_3O_{6.25}$ are closely related to oxygen ordering. They ascribed this relation to a charge-transfer mechanism, similarly to what is believed to happen in the orthorhombic phase. We shall assume that this close relation between the electronic properties and oxygen order occurs also in the high-temperature region of the tetragonal YBCO phase diagram.

We now discuss the origin of the long-time relaxation processes. Although, curves shown in Figs. 4 and 5 are obtained at a very low oxygen partial pressure (<10 ppm), one may argue that the oxygen stoichiometry can change during a temperature sweep. Combined TGA and resistance measurements show that bulk oxygen diffusion occurs in a time

scale that is much shorter (2 orders of magnitude) than resistance relaxation. Therefore we have to assume that another process occurs in a time scale longer than bulk oxygen diffusion. Based on the structural studies mentioned before, we propose that long relaxation time is due to oxygen ordering (or disordering) within the tetragonal YBCO structure. The long-time scale at which these processes occur is characteristic of a special class of oxides (which tetragonal YBCO probably belongs to) whose origin is related to the competition among metastable phases. Material stability is indeed given by a shallow minimum of the free energy $G(T,x,\ldots) = H - TS = (U + PV) - TS$ that is a function of physical $(T,P,V,...)$ and chemical (oxygen concentration x, oxygen ordering,...) parameters. Enthalpy H is usually the dominant term and it has well-defined minima which provide stable atom configurations. However, in a special class of oxides, including $Fe_{1-x}O$ and CeO_{2-x}, the entropy term S may dominate, especially at high temperatures, and in such a case the free energy gets a broad shape typical of entropy S. In these materials, known as nonstoichiometric oxides, different oxygen configurations are allowed. The origin of this peculiarity is related to the mixed valence of metals (Fe, Ce,...), i.e., the possibility to assume different oxidation states.[26] In the family of $YBa_2Cu_3O_{6+x}$ there are two stoichiometric phases, obtained for $x=0$ and 1, in which there are neither defects or vacancies of oxygen (chains are completely full or empty). It has been pointed out, however, that oxygen defects (vacancies) may assume different equivalent coordinations when $x<0.5$ in $YBa_2Cu_3O_{6+x}$ and this increases the entropy contribution[11] (there are 4 equivalent positions in the CuO basal planes for oxygen defects in the tetragonal phase instead of 2 in the orthorhombic one). Long relaxation time is required in order to find a configuration with favorable energy conditions. In a previous work we have shown that the relaxation time needed to achieve a steady state can actually be modified by changing the metal valence in qualitative agreement with this model.[12] In the last few years, time-dependent phenomena, such as photoinduced electrical changes[14–16] as well as structural modifications occurring in the time scale of several minutes,[17] have been observed in oxygen-deficient YBCO at room temperature. In Fig. 4(c) we have shown that the R vs T curve depends on the thermal cycle even below 200 °C. This suggests that different time-dependent phenomena have the same origin and they occur in a wide region of temperature and oxygen concentration.

In the following we discuss the maximum of the R vs T curve shown in Figs. 2 and 3. We first point out that, despite the high oxygen mobility, the ion conductivity is smaller than the electronic one, hence the latter is the dominant contribution to charge transport even at high temperatures.[27] Grader *et al.*[3] interpret the resistance bump as a metal - nonmetal transition. We report here further experiments that may better clarify this issue. In Fig. 3 we note that the steady-state resistance increases as temperature increases from 500 °C to 650 °C suggesting a metallic behavior. We point out, however, that all samples treated at $T_p \geqslant 500$ °C for a long time exhibit cycle-dependent resistance during the following slow cooling, i.e., the behavior is similar to that reported in Fig. 4. Further, we note that the slope of R vs T is actually slightly positive (metal-like) for $T_p = 500$ °C yet samples treated at 600 °C show cooling R vs T curves quite similar to those reported in Fig. 4 with both positive and negative slopes. In this case the classification as a metal is meaningless, although we deal with samples treated below the maximum of the curve reported in Fig. 3. In order to characterize the resistance behavior above 650 °C, we performed further measurements in samples treated up to 820 °C following the procedure of Fig. 1(a). Resistance measurements were taken during a quick cooling, i.e., the oven cooling time which is ~20 min to get 600 °C from 820 °C. Plotting the resistance as a function of $1/T$ in a semilog scale we found straight lines with different slopes (i.e., activation energies E_0) in samples heated at different rates. Activation energy values found in such a way are different from what we found taking the steady-state resistance values: in this case we measured $E_0 = 1.2$ eV while measurements on quenching give activation energy ranging between 0.2 and 0.8 eV. Note that E_0 obtained from high-temperature resistance ranges from 0.1 to 0.7 eV in data reported in the literature.[6] These results show that above 650 °C the resistance behavior is actually thermally activated (semiconductorlike) even when different thermal procedures are followed. However, we conclude from these experiments that the resistance maximum shown in Fig. 3 cannot be simply considered as a sharp metal-nonmetal transition occurring at a given temperature (650 °C) in a stoichiometric compound. In other words, we have also to take into account the resistance dependence on oxygen concentration and/or oxygen order. We expect indeed that oxygen defects strongly determine the charge carrier hopping mechanism by changing both the density of electronic states and the hopping length (energy). The concentration and the order of oxygen defects change as temperature changes and, according to what we discussed before, these structural modifications depend on the preceding thermal path. Hence we believe that the shape of the R vs T curve reported in Fig. 3 mainly reflects structural changes which occur continuously above 500 °C. This model may also account for the wide spread results found in the literature and in our experiments. We can hardly distinguish whether the major effects of structural modifications are on the density of electronic states or in the hopping length. However, it is worth reminding the reader that we found that oxygen slightly decreases from 6.2 to 6.1 per u.f. as the temperature increases from 500 °C to ~600 °C. It is likely that the resistance increase is essentially due to a decrease of the density of electronic states in this temperature range. We just note that this is consistent with early Hall effect experiments.[28] At higher temperatures ($T>650$ °C) the oxygen content is reduced to a very little, and probably ultimates, value (6.1 per u.f.) and it is likely that the charge-transfer mechanism is less efficacious. Carrier hopping is thermally activated, yet oxygen order may determine the characteristic activation energy by changing, mainly, the hopping length in this temperature range.

In conclusion we have studied the high-temperature resistance of tetragonal $YBa_2Cu_3O_{6+x}$ following different experimental procedures. Our experiments show that there are two main features of the resistance at high temperature: (1) a long relaxation time (typically $\sim 10^3$ min at 650 °C) is required to get a steady resistance value; (2) the steady-state resistance plotted as a function of temperature exhibits a maximum at ~650 °C. Comparison of resistivity and thermogrametric

measurements taken at the same conditions shows that oxygen diffusion occurs in a time scale much shorter than the achievement of steady resistance. We proposed that the long relaxation time observed in resistivity measurements are related to oxygen ordering (or disordering) and we discuss the resistance maximum in terms of the nonstoichiometry of the YBCO tetragonal phase. Our observations may help to account for controversial results reported in the literature (for example the activation energy of charge transport in tetragonal YBCO) and they suggest that time-dependent phenomena occur in a wide region of tetragonal YBCO phase diagram.

ACKNOWLEDGMENTS

We thank G. Boara for the oxygen determination and S. Bertoni and C. Bucci for the SEM micrographs. We are grateful to A. Migliori (Istituto di Chimica e Tecnologia dei Materiali e Componenti per l'Elettronica del C.N.R., Bologna, Italy) who performed electron-diffraction patterns.

[1] E. T. Heyen, J. Kirker, and M. Cardona, Phys. Rev. B **45**, 3037 (1992).
[2] T. K. Chaki and M. Rubestein, Phys. Rev. B **36**, 7259 (1987).
[3] G. Sageev Grader, P. K. Gallagher, and E. M. Gyorgy, Appl. Phys. Lett. **51**, 1115 (1987).
[4] A. T. Fiory, M. Gurvitch, J. R. Cava, and G. P. Espinosa, Phys. Rev. B **36**, 7262 (1987).
[5] J. S. Park and H. G. Kim, Jpn. J. Appl. Phys. **27**, L191 (1988).
[6] P. P. Freitas and T. S. Plaskett, Phys. Rev. B **37**, 3657 (1988).
[7] J. Genossar, B. Fisher, I. O. Lelong, Y. Ashkenazi, and L. Patlagan, Physica C **157**, 320 (1989).
[8] H. Ishizuka, Y. Idemoto, and K. Fueki, Physica C **195**, 145 (1992).
[9] E. K. Chang, D. J. L. Hong, A. Metha, and D. M. Smyth, Mater. Lett. **6**, 251 (1988).
[10] H. I. Yoo, J. Mater. Res. **4**, 23 (1989).
[11] J. Nowotny, J. Am. Ceram. Soc. **73**, 1040 (1990).
[12] M. Affronte, C. Nobili, G. Ottaviani, and F. Licci, Physica C **234**, 91 (1994).
[13] J. D. Jorgensen, S. Pey, P. Lightfoot, H. Shi, A. P. Paulikas, and B. W. Veal, Physica C **167**, 571 (1990).
[14] G. Nieva, E. Osquiguil, J. Guimpel, M. Maehoudt, B. Wuyts, Y. Bruyseraede, M. P. Maple, and I. K. Schuller, Phys. Rev. B **46**, 14 249 (1992).
[15] K. Kawamoto and I. Hirabayashi, Phys. Rev. B **49**, 3655 (1994).
[16] K. Tanabe, S. Kubo, Hosseini Teherani, H. Asano, and M. Suzuki, Phys. Rev. Lett. **72**, 1537 (1994).
[17] H. Shaked, J. D. Jorgensen, B. A. Hunter, R. L. Hitterman, A. P. Paulikas, and B. W. Veal, Phys. Rev. B **51**, 547 (1995).
[18] S. Semenovskaya and A. G. Khachaturyan, Phys. Rev. B **46**, 6511 (1992).
[19] A. A. Aligia and J. Garcés, Phys. Rev. B **49**, 524 (1994).
[20] G. Boara and M. Sparpaglione (private communication).
[21] C. Nobili, G. Ottaviani, M. C. Rossi, and M. Sparaglione, Physica C **168**, 594 (1990).
[22] S. J. Rothman, J. L. Routbort, U. Welp, and J. E. Baker, Phys. Rev. B **44**, 2326 (1991), and references therein.
[23] T. Matsui, K. Naito, and S. Hagino (unpublished).
[24] P. G. Radaelli, C. U. Segre, D. G. Hinks, and J. D. Jorgensen, Phys. Rev. B **45**, 4923 (1992).
[25] R. Sonntag, D. Hohlwein, T. Brukel, and G. Collin, Phys. Rev. Lett. **66**, 1497 (1994).
[26] See, for example, *Nonstoichiometric Oxides*, edited by O. T. Sørensen (Academic, New York, 1981).
[27] The ion conductivity can be extimated using the thermal diffusion coefficient D_0. Using the Einstein relation $\sigma=e^2ND_0(k_BT)^{-1}$ and taking $T=900$ K, $N\sim(173\ \text{Å}^3)^{-1}$ as carrier density, $D_0=4\times10^{-9}\ \text{cm}^2\,\text{s}^{-1}$ we find that the ion contribution to resistivity $\rho_{\text{ion}}=\sigma^{-1}$ at $\sim630\,^\circ\text{C}$ is $\rho_{\text{ion}}=0.7\times10^4\ \Omega\,\text{cm}$, while the electron resistivity is $\rho_{\text{el}}=\rho_0R/R_0\sim10^{-1}\ \Omega\,\text{cm}$ taking $\rho_0=10^{-4}\ \Omega\,\text{cm}$ and $R/R_0=10^3$, that is $\rho_{\text{el}}\ll\rho_{\text{ion}}$.
[28] G. S. Grader, P. K. Gallagher, and A. T. Fiory, Phys. Rev. B **38**, 844 (1988).